Neurosurgical Review (2026) 49:96
https://doi.org/10.1007/s10143-025-04040-9

RESEARCH

Retrosigmoid transtentorial approach for accessing the mediobasal temporal region: a radiological and anatomical evaluation

Muhammet Elveren[1] · Ufuk Temtek[1] · Nuh Çağrı Karaavcı[1] · Mehmet Emin Akyüz[2] · Mete Zeynal[2] · Caner Fahrettin Kara[3] · Samet Kapakin[4] · Ahmet Yalçın[5] · Hakan Hadi Kadıoğlu[2] · Mehmet Hakan Şahin[6]

Received: 28 August 2025 / Revised: 4 November 2025 / Accepted: 10 December 2025

Abstract

The study assesses the retrosigmoid transtentorial approach for accessing the mediobasal temporal region, hypothesizing benefits such as a shorter surgical path, reduced tissue trauma and improved ergonomic feasibility. It aims to anatomically validate the approach, compare it with existing techniques, and detail predictive radiological metrics to foresee surgical challenges, emphasizing its advantages. In eight cadaveric specimens and 100 brain imaging studies without reported cranial pathology, the tentorial and occipital angles, as well as the distances between the retrosigmoid entry point and key landmarks of the mediobasal temporal region including the temporal pole, temporal horn, and inferior choroidal point were measured. The cadaveric dissections were documented photographically, and the inferomedial exposure of the mediobasal temporal region through the retrosigmoid transtentorial approach was evaluated. The anatomical limitations of this approach were identified, and its surgical safety, advantages, and drawbacks were compared with those of existing approaches. Radiological analysis of the 100 brain MRIs revealed a mean tentorial angle of 41.76° ± 6.8° and an occipital angle of 114.7° ± 8.4°. The average distances from the retrosigmoid entry point (REP) to key anatomical landmarks were as follows: to the temporal pole (TmP), 88.22 ± 9.6 mm; to the temporal horn (Th), 63.84 ± 6.1 mm; and to the inferior choroidal point (IchP), 64.67 ± 6.08 mm. Cadaveric measurements yielded similar findings. The mean tentorial angle was 36.88° ± 4.2° and the occipital angle was 108.86° ± 4.1°. The distances from REP to IchP, Th, and TmP were 68.93 ± 6.8 mm, 68.29 ± 6.6 mm, and 85.21 ± 5.8 mm, respectively.

Keywords Retrosigmoid transtentorial approach · Mediobasal temporal region · Temporal lobe surgery · Anatomical dissection · Cadaveric study. neuroanatomy

Introduction

The mediobasal temporal region (MTR), a component of the limbic lobe, lies above the tentorium cerebelli and curves around the brainstem. Temporal lobe epilepsy surgery aims to halt seizures, preserve memory, prevent additional neurological deficits, and improve quality of life [1].

Evaluation of surgical techniques for this region reveals specific advantages and limitations for each, with no universally accepted approach. The choice of technique generally depends on the surgeon's experience and familiarity. Complete access to the MTR may necessitate multiple or combined procedures, as a single approach may not be sufficient [2–6].

This study aimed to investigate the potential of the retrosigmoid transtentorial approach (RSTTA), a technique traditionally employed for petroclival lesions and ventrolateral

✉ Muhammet Elveren
dr.muhammetelveren@gmail.com

1 Department of Neurosurgery, University of Health Sciences, Erzurum Regional Training and Research Hospital, Erzurum, Turkey

2 Department of Neurosurgery, Faculty of Medicine, Erzurum Atatürk University, Erzurum, Turkey

3 Department of Neurosurgery, Giresun Training and Research Hospital, Giresun, Turkey

4 Department of Anatomy, Faculty of Medicine, Erzurum Atatürk University, Erzurum, Turkey

5 Department of Radiology, Faculty of Medicine, Erzurum Atatürk University, Erzurum, Turkey

6 Department of Neurosurgery, Medicana International Samsun Hospital, Samsun, Türkiye, Turkey

Published online: 03 January 2026

brainstem access, for reaching the MTR. It was hypothesized that this approach might offer a shorter surgical corridor, reduce trauma to surrounding tissues, and increase procedural comfort for both the patient and the surgeon. The objectives were to anatomically validate this surgical pathway, compare it with established techniques, and define radiological metrics that could help predict the preoperative accessibility of the entire MTR. Ultimately, this study sought to provide new insights into the applicability of RSTTA for MTR access and to highlight its potential advantages.

Material and method

This study was performed as a scientific research project in the Erzurum Atatürk University Neuroanatomy Laboratory between 2022 and 2023, after receiving approval from the Ethics Committee of Erzurum Atatürk University (approval code, TTU-2022-10480). To ensure that the study results remained unaffected, eight cadavers (mean age, 72.1 ± 5.02 years) prepared using the Klingler method were used. None of the cadavers had a cause of death attributed to cranial pathology [7]. The cadaver heads, preserved in a 70% alcohol solution, were thoroughly rinsed with tap water. Imaging was then performed using a Toshiba TSX-301 C computed tomography (CT) device and a Siemens Magnetom Skyra 3.0T magnetic resonance imaging (MRI) device, producing 1-millimeter, isotropic sequences in three orthogonal anatomical planes. All MRI studies were acquired using 1-mm isotropic T1-weighted and T2-weighted sequences to allow accurate multiplanar reconstructions. CT scans were reconstructed with 1-mm isotropic voxels. These imaging parameters were selected to ensure precise measurement of tentorial and occipital angles and reliable localization of the retrosigmoid entry point. As shown in Fig. 1, tentorial angles (TA), occipital angles (OA), and the distances between the retrosigmoid entry point (REP) and key landmarks of the mediobasal temporal region, including the temporal pole (TmP), temporal horn (Th), and inferior choroidal point (IchP), were measured on MRI and CT images (Fig. 1). The tentorial angle (TA) was defined as the angle between the tentorium cerebelli and the clivus on the midsagittal plane. The occipital angle (OA) was defined as the angle formed between the inferior surface of the occipital lobe and the tentorial surface. The retrosigmoid entry point (REP) was identified as the intersection of a line drawn 2 cm medial to the transverse–sigmoid junction with the inferior border of the transverse sinus. TA and OA measurements were performed on midsagittal MRI images using digital angle-calculation tools. Lines forming the tentorial surface and the clival or occipital surfaces were manually identified, and angles were calculated automatically by the software. REP-related measurements were performed on axial CT and MRI images, using the REP point as a fixed origin. Distances to the temporal pole, ambient cistern, and other key landmarks were obtained using electronic calipers with 1-mm precision. To avoid measurement errors related to head positioning, all cadaveric specimens were aligned in a neutral sagittal plane before imaging. The hard palate and the cranial base served as anatomical reference lines to ensure that no flexion or extension tilt was present. Axial datasets were used only after confirming that the midsagittal plane was orthogonal to the axial slices. Following image integration into the neuronavigation system, the cadavers were positioned for surgical guidance in the Fukushima position (three-quarter prone) using a three-pin skull clamp (Figs. 2 and 3A) [8]. A neuronavigation system (Brainlab Buzz 2.0, Munich, Germany), equipped with a 42-inch Full HD touchscreen interface, was used during cadaveric positioning and trajectory planning to correlate anatomical landmarks with radiological measurements. Additionally, brain images were obtained from a sample of 100 patients, consisting of 50 males and 50 females without any cranial pathology, as confirmed by hospital records.

The measurements were followed by dissection. To accurately access the target area using the planned surgical approach, a wide incision was performed to expose both the supratentorial and infratentorial regions. The scalp was elevated while preserving the sagittal suture on the medial side and the auricle on the lateral side (Fig. 3B). The galea and periosteum were retracted sequentially (Fig. 3C). Bone tissue was excised using an electric cutter, with careful preservation of both the sagittal suture and the lambdoid suture to serve as landmarks (Fig. 3D). The transverse sinus and sigmoid sinus were preserved, whereas the dura mater was removed (Fig. 3E). The upper one-third of the cerebellum was removed to demonstrate the cerebellar relaxation in the cadaver resulting from cerebrospinal fluid (CSF) drainage from the cisterna magna during surgery and provide a more demonstrative view from the inferomedial angle. Subsequently, following the falx cerebri, the right hemisphere of the cerebrum was removed by entering through the middle of the corpus callosum and cutting through the middle part of the mesencephalon, with the thalamus remaining medially (Fig. 3F).

The anatomical structures on the removed hemisphere were identified and the hemisphere was repositioned after marking the lingual gyrus, parahippocampal gyrus, fusiform gyrus, and collateral sulcus with colored markers to serve as surgical guides (Fig. 4A). The tentorium was incised in a U-shape from its free edge, with the base directed toward the transverse sinus and the opening facing the lingual gyrus, parahippocampal gyrus and fusiform gyrus (Fig. 5A and B). This approach facilitated the identification of anatomical

MEASUREMENTS		PLANE	DEFINITION	VISUAL
ANGLE MEASUREMENT	Tentorial angle (TA)	Sagittal	Tentorial angle (a) measured between the TCb and a line (Twining line) from the internal occipital protuberance (iop) to the tuberculum sellae (tus)	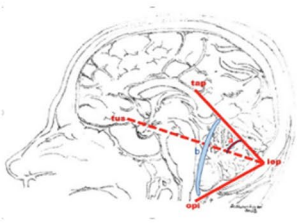
	Occipital angle (OA)	Sagittal	Occipital angle (b) between the TCb and the line connecting the iop and the opisthion (opi)	
SURGICAL DISTANCE MEASUREMENT	**Distance from the REP to the IchP	Axial	Distance between the REP and the inferior choroidal point (IchP), which is the entry point of the inferior choroidal artery into the temporal horn	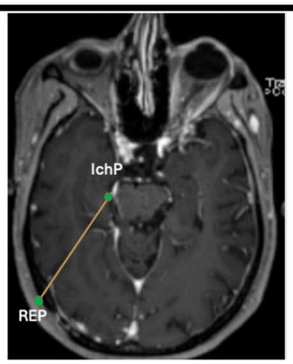
	Distance from the REP to the Th	Axial	Distance between the REP and the most anterior visible part of the temporal horn (Th)	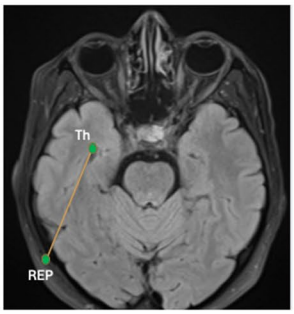
	Distance from the REP to the TmP	Axial	Distance between the REP and the temporal pole (TmP)	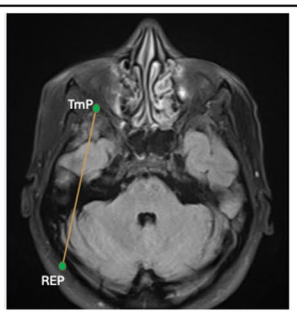

Fig. 1 Measurements and definitions on radiological images. Retrosigmoid entry point (REP): The intersection of the lower edge of the transverse sinus and two cm medial to the junction of the transverse sinus and the sigmoid sinus. TCb: Tentorium cerebelli

structures visible through the tentorial incision (Fig. 4B). Subpial dissection was then performed anteriorly using a Cavitron Ultrasonic Surgical Aspirator (CUSA) through an incision made on the parahippocampal gyrus at the branching point of the posterior cerebral artery (Fig. 4C). The tail of the hippocampus was resected anteriorly, leaving the posterior cerebral artery medially and the collateral sulcus laterally. The hippocampal body and most of the head were resected by extending the dissection superiorly and medially until reaching the temporal horn of the lateral

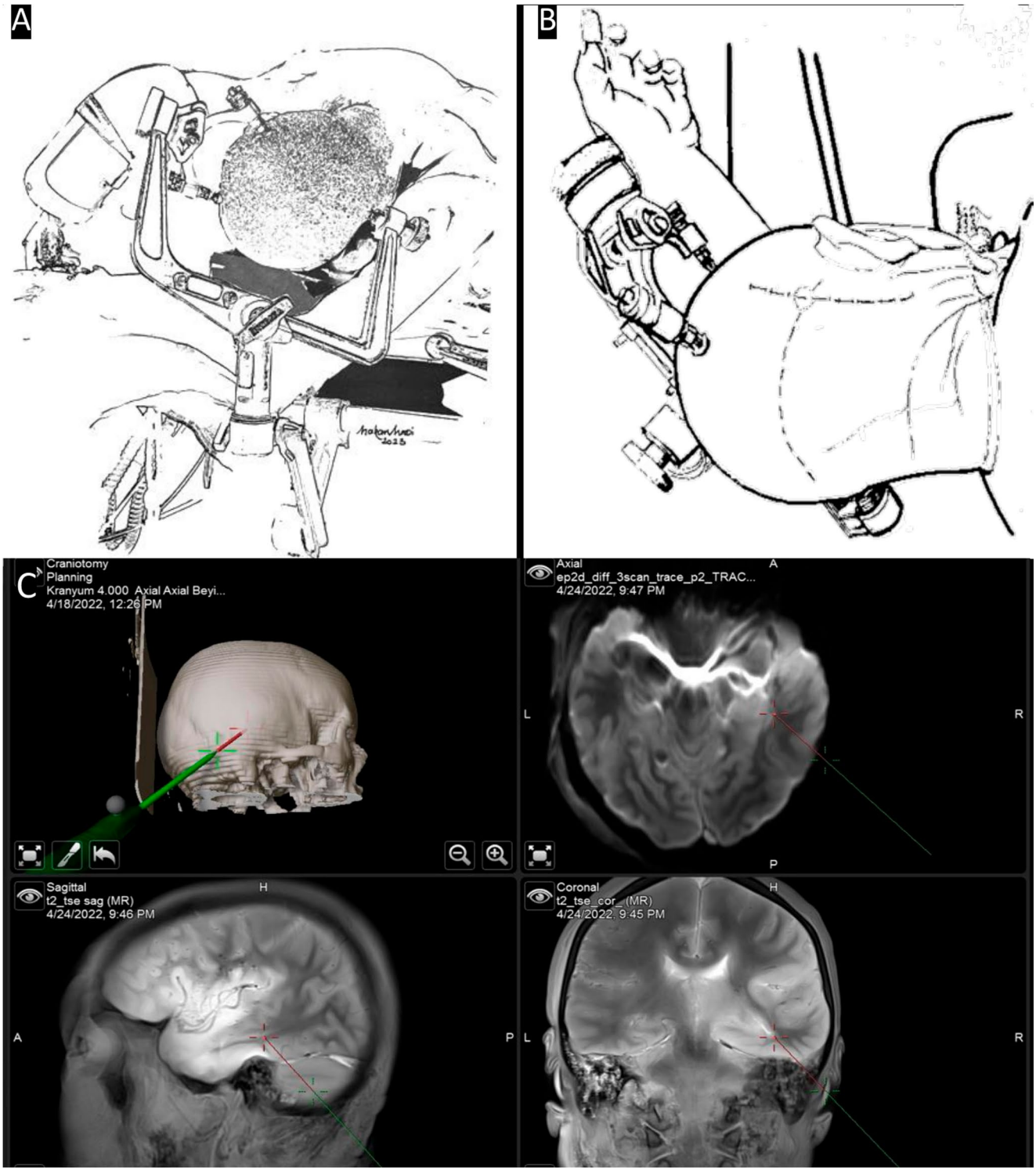

Fig. 2 (**A**, **B**) Schematic view of Fukushima position using a three-pin skull clamp. (**C**) Neuronavigation system showing the surgical direction from the REP to the MTR in axial, sagittal, and coronal planes, respectively

ventricle, located approximately two and a half centimeters distally. During this procedure, approximately a 2-cm segment of the fusiform gyrus was included in the resection to ensure a favorable visual angle. To expose the ventricular structures, the dissection was gently extended over the lateral aspect of the anterior temporal pole, which provided a direct view of the temporal horn and subsequently the choroid plexus (Fig. 6A). The dissection was extended laterally

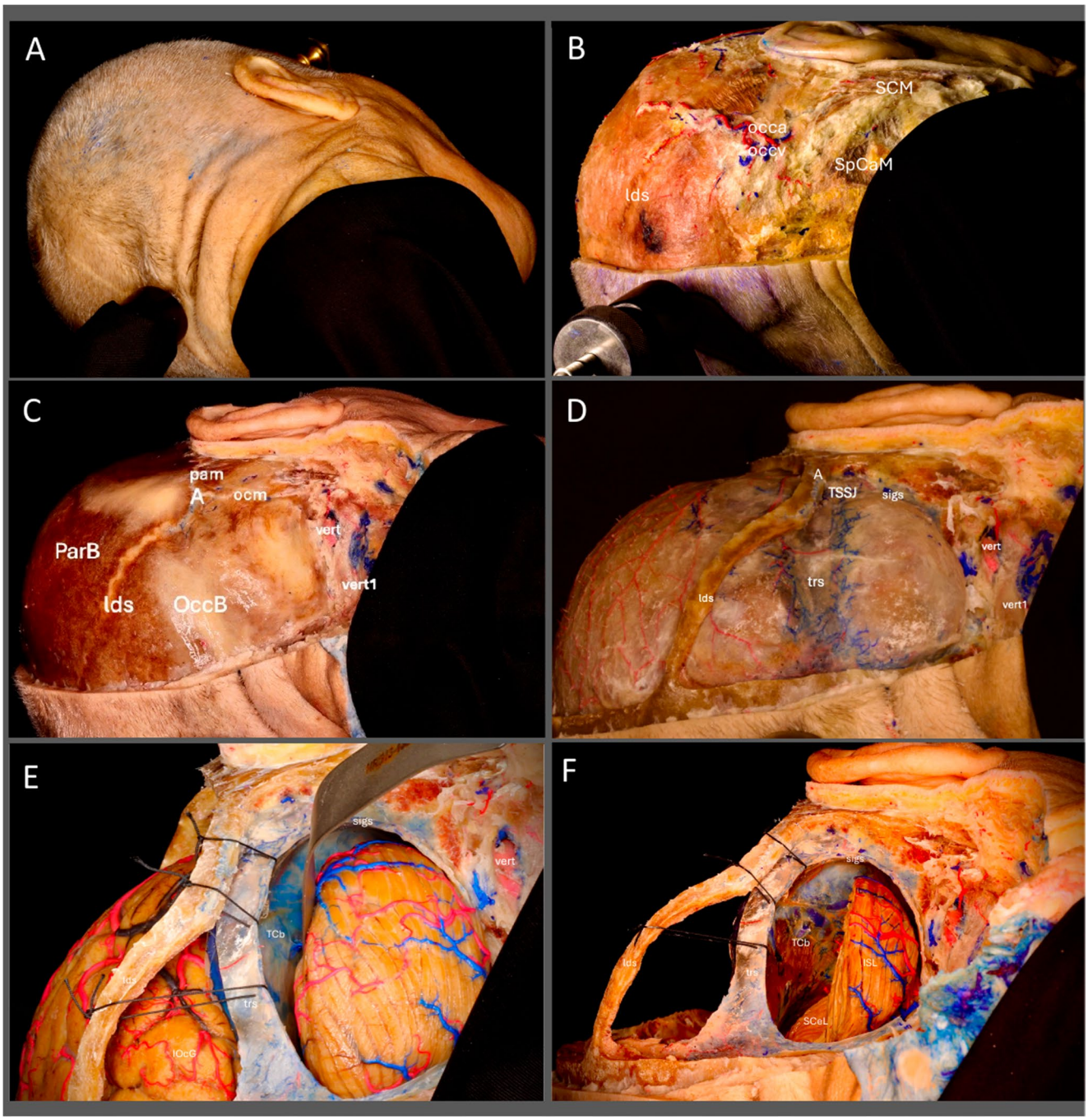

Fig. 3 (**A**) Demonstration of fixation of the head specimen with a 3-pin fixator and positioning according to Fukushima. (**B**) Image after removing the scalp with the sagittal suture on the medial side and the auricle border on the lateral side. (**C**) View of the cranium after muscle and periosteum removal. (**D**) Removal of the bone with preservation of the lambdoid suture and exposure of the dura, (**E**) Removal of the dura with preservation of the transverse and sigmoid sinus and exposure of the cerebellum, (**F**) Cutting the upper 1/3 of the cerebellum and the right hemisphere for a wider view and exposure of anatomical landmarks (A; asterion, ISL; inferior cerebellar lobule, lds; lambdoid suture, occa; occipital artery, ocm; occipito- mastoid suture, OccB; occipital bone, occv; occipital vein, SCM; sternocleidomastoid muscle, pam; parieto-mastoid suture, ParB; parietal bone, SCel; superior semilunar lobule, sigs; sigmoid sinus, SpCaM; splenius capitis muscle, Tcb; tentorium cerebelli, TSSJ; transvers sinus- sigmoid sinus junction, trs; transverse sinus, vert; vertebral artery)

and inferiorly from the lateral wall until the internal cerebral artery and the optic nerve became visible, and the amygdala and the remaining portion of the head of the hippocampus were resected (Fig. 6B). The resection was performed with the fusiform gyrus remaining on the lateral side, the posterior cerebral artery and its branches on the medial side, the

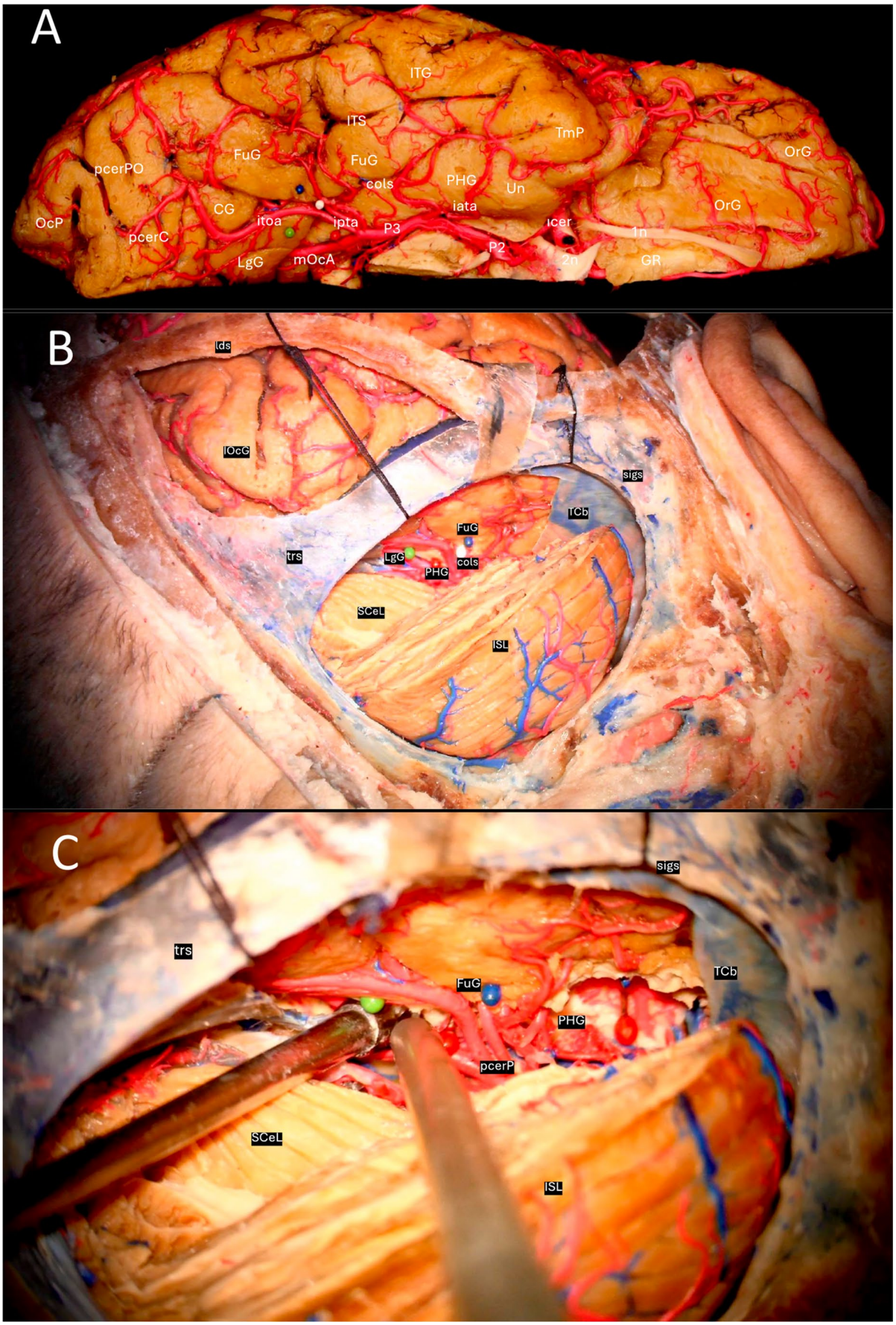
A
ITG
ITS
TmP
OrG
pcerPO
FuG
FuG
cols
PHG
Un
iata
OrG
CG
itoa
ipta
P3
icer
1n
OcP
pcerC
P2
2n
GR
LgG
mOcA
B
lds
lOcG
sigs
TCb
FuG
trs
LgG
cols
PHG
SCeL
lSL
C
sigs
trs
TCb
FuG
PHG
pcerP
SCeL
lSL

Fig. 4 (**A**) Image of the inferior surface of the right hemisphere removed from the cranium to provide topographic dominance, with pins marking the cortical areas associated with the surgical approach, blue pin; fusiform gyrus, green pin; lingual gyrus, white pin; collateral sulcus, red pin; parahippocampal gyrus. (**B**) The image obtained from the tentorium incision after the replacement of the hemisphere with cortical markers. (**C**) Subpial resection with the help of CUSA, starting from the posterior cerebral artery P3 branch point

anterior one-third of the uncus anteriorly, and the lingual gyrus posteriorly (Fig. 6C). Photographs were recorded at every stage of the dissection process.

All collected data were subjected to statistical analysis using IBM SPSS Version 25.0 (IBM Corp., Armonk, NY) software. Data were expressed as frequency (percentage), mean, and standard deviation. The chi-square (χ^2) test was used to analyze categorical data, while the Student's t-test was used to compare angle and distance measurements. A p-value of less than 0.05 was considered statistically significant. The Pearson correlation test was employed to determine the relationships between all calculated values. Correlation coefficients (r values) were interpreted as follows: 0–0.25, very weak correlation; 0.26–0.49, weak correlation; 0.50–0.69, moderate correlation; 0.70–0.89, strong correlation; and >0.90, very strong correlation.

Results

Radiological analysis of the eight cadaveric specimens revealed that the tentorial angle (TA) ranged from 32.3° to 43.8° (mean±SD, 36.88° ± 4.2°) and the occipital angle (OA) ranged from 104.7° to 116.4° (mean±SD, 108.86° ± 4.1°). The measured distances from the retrosigmoid entry point (REP) to key anatomical landmarks were as follows: from REP to the inferior choroidal point (IchP) ranged from 59.51 mm to 78.32 mm (mean±SD, 68.93±6.8 mm); from REP to the temporal horn (Th) ranged from 59.42 mm to 77.86 mm (mean±SD, 68.29±6.6 mm); and from REP to the temporal pole (TmP) ranged from 74.32 mm to 92.54 mm (mean±SD, 85.21±5.8 mm) (Table 1).

In the 100 brain MRI scans of individuals without cranial pathology, the tentorial angle ranged from 25.6° to 52.6° (mean±SD, 41.76° ± 6.8°), and the occipital angle ranged from 96.7° to 131.7° (mean±SD, 114.7° ± 8.4°). Distances from the REP to key landmarks were as follows: to the IchP, 53.39–79.98 mm (mean±SD, 64.67±6.08 mm); to the Th, 52.85–79.13 mm (mean±SD, 63.84±6.1 mm); and to the TmP, 73.57–119.17 mm (mean±SD, 88.22±9.6 mm) (Table 1).

Analysis revealed a strong positive correlation between the tentorial angle and the occipital angle ($r=0.973$, $p<0.001$). Additionally, moderate positive correlations were observed between the tentorial angle and the distances from REP to IchP ($r=0.305$, $p=0.02$), REP to Th ($r=0.301$, $p=0.02$), and REP to TmP ($r=0.358$, $p=0.01$). Similarly, the occipital angle showed moderate positive correlations with the distances from REP to IchP ($r=0.294$, $p=0.03$), REP to Th ($r=0.292$, $p=0.03$), and REP to TmP ($r=0.346$, $p=0.01$). Moreover, strong positive correlations were found among distance measurements: REP–IchP and REP–Th ($r=0.996$, $p<0.001$), REP and TmP ($r=0.798$, $p<0.001$), and REP–Th and REP–TmP ($r=0.790$, $p<0.001$) (Table 2).

Discussion

Located near critical neurovascular structures, the MTR is susceptible to various pathologies. Surgical goals include removing the pathology with minimal damage, ideally in one session. Challenges arise from the MTR's deep location, its elongated shape, and the adjacent temporal and occipital neocortices, complicating surgery [3]. Approaches to the surgery of vascular and tumoral lesions located in the MTR are typically chosen according to the long axis of the temporal lobe (Table 3).

Although several studies have examined various routes to the mediobasal temporal region, none have combined radiological measurements with cadaveric dissection to evaluate the anatomical feasibility of the retrosigmoid transtentorial approach. The present study is novel in that it correlates tentorial and occipital angles with anterior mediobasal temporal accessibility, and proposes angle-based radiological predictors for determining when endoscopic assistance may become necessary. This integrated radiological–anatomical analysis has not been previously reported in the literature.

Some surgeons prefer to perform anterior temporal lobectomy or anteromedial temporal lobectomy in MTR surgery [9, 10]. In the literature, hemiparesis and language disorders are among the most serious complications occurring after anterior temporal lobectomy [11–18]. The transsylvian approach, demonstrated accessibility to the anterior and middle parts of the MTR without the need for neocortical resection [19, 20]. This approach requires precise surgical control, and a risk of encountering vascular injuries during the procedure exists. Furthermore, when extending posteriorly, it is highly probable that the temporal cortex and optic radiation may get damaged [4]. An additional concern regarding the transsylvian approach is the potential transgression of the temporal stem, which contains critical fronto-temporal associative fibers [21]. Previous anatomical and functional studies have demonstrated that injury to the temporal stem may result in language, semantic, and memory-related disturbances, particularly when deep dissection is required to reach mesial temporal structures [22–24]. This structural vulnerability represents a limitation of the

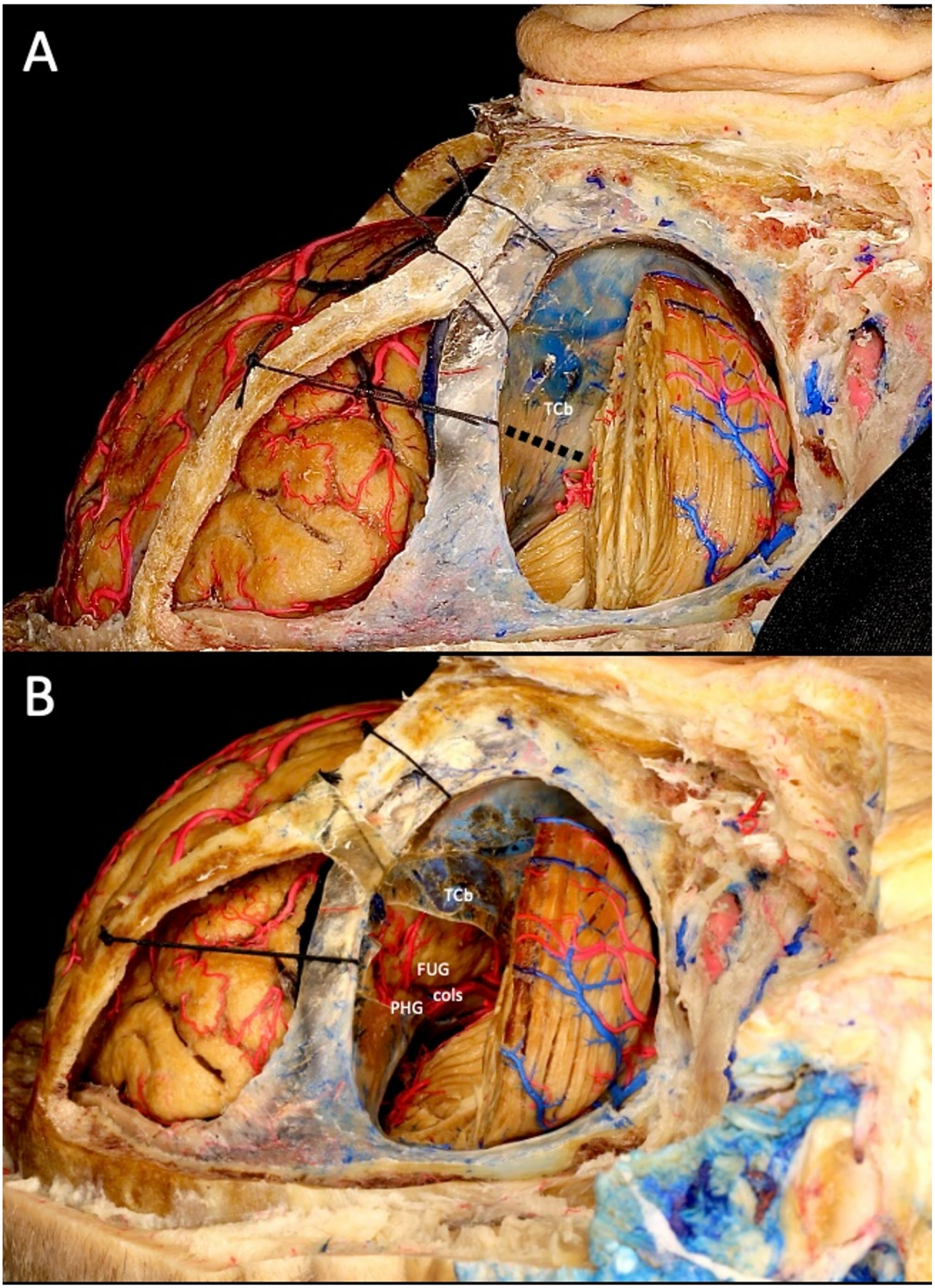
A
TCb
B
TCb
FUG
cols
PHG

Fig. 5 (**A**) Schematic demonstration of the tentorial incision performed through the retrosigmoid transtentorial approach. The orientation, extent, and direction of the tentorial cut are illustrated, showing how division of the tentorium cerebelli widens the operative window toward the mediobasal temporal region. TCb; tentorium cerebelli. (**B**) View through the tentorial opening after division of the tentorium cerebelli. The expanded surgical corridor reveals key mediobasal temporal structures. The figure demonstrates the increase in exposure achieved following tentorial incision. PHG; parahippocampal gyrus, cols; collateral sulcus, FUG; fusiform gyrus, TCb; tentorium cerebelli

transsylvian route when targeting the mediobasal temporal region. In contrast, the retrosigmoid transtentorial approach does not traverse the temporal stem, thereby avoiding injury to these essential white-matter pathways .

Approaches to the basal and lateral surfaces are other alternatives to access the MTR and can be further divided into subtemporal and transsulcal approaches to the basal surface, and transsulcal and transgyral approaches to the lateral surface. All of these approaches have limitations in terms of exposing the full extent of the MTR and require temporal lobe retraction or incisions, which can potentially compromise optic radiation [4]. A further limitation of the subtemporal approach is the vulnerability of the venous drainage system, particularly the vein of Labbe and adjacent bridging veins. Elevation of the temporal lobe may stretch or occlude these veins, predisposing patients to venous infarction, edema, and postoperative neurological deficits [25, 26]. This venous risk represents a major constraint when working through the subtemporal corridor. In contrast, the retrosigmoid transtentorial approach avoids temporal lobe retraction and therefore minimizes the likelihood of venous injury.

The occipital interhemispheric approach is primarily used for posterior MTR lesions. Additionally, for similar lesion locations, the supratentorial infraoccipital and lateral occipital subtemporal approaches are options. These methods offer posterior access, extending potentially to the MTR's middle. However, they may necessitate significant occipital lobe retraction, posing risks to occipital, basal, and posterior temporal veins [2, 27–29].

The PST approach to the medial surface is advantageous as it avoids damage to the lateral cortex, basal cortex, and optic radiation. However, it is limited to the posterior and middle parts of the MTR and requires cerebellar retraction. Additionally, the seated position requirement may lead to surgeon fatigue during the operation [2].

RSTTA, like the PST approach, is less likely to cause post-surgical visual field defects compared to traditional methods. Literature cites successful pterional-transsylvian surgeries without visual complications. Yet, some surgeons report visual deficits, likely due to a lesser understanding of the required microsurgical techniques and anatomy [19, 20, 22–24, 30–34]. In these approaches, the surgical corridor is not in close proximity to the visual cortex and optic radiation, thereby minimizing the likelihood of injury to these structures.

RSTTA and PST methods avoid complications like atrophy, mastication problems, and cosmetic issues that the superior, medial, and basal approaches pose due to potential damage to the frontal facial nerve branches. Yet, they require caution to prevent harm to the occipital artery, vein, and nerve [4, 35].

It is evident that the advantages and disadvantages of PST and RSTT approaches are quite similar compared to other surgical methods. However, the PST approach provides access to the posterior and middle parts of the MTR, while the anterior part requires endoscope support. Depending on the surgeon's experience and mastery of microsurgical anatomy, using this approach to access all parts of the MTR may be feasible. Accessing the MTR using the RSTTA is influenced by the tentorial angle (TA). A study in the literature indicated that decreased TA led to a decrease in occipital angle (OA), and conversely, an increased TA was associated with reduced control over the MTR, particularly its anterior portion. In our study, both the OA and TA were measured using cranial MRIs from cadavers and 100 cases, and compared. The Pearson correlation test showed a strong positive relationship between TA and OA ($r = 0.973$, $p < 0.05$), meaning TA increases coincided with rises in OA. Using RSTTA, we accessed the entire MTR in cadavers with lower TAs. In two cadavers with higher TAs, anterior MTR resections were successfully performed with the assistance of an endoscope. Additionally, seeing the fusiform gyrus (FuG) in the surgical view could ease reaching masses or vascular malformations in this region .

The sitting position has traditionally played an important role in posterior fossa and pineal region surgery, providing excellent gravitational retraction and versatile working angles. Modern studies have shown that when appropriate safety protocols are applied—including modified sitting positions, antigravity trousers, intraoperative Doppler monitoring, and optimized anesthetic management—the risk of venous air embolism can be significantly reduced [8, 36–41]. In our cadaveric study, the Fukushima three-quarter prone position was preferred primarily for ergonomic reasons. Furthermore, if intraoperative ultrasound (USG) imaging is required, filling the operative corridor with irrigation fluid is more practical in this position, as gravity keeps the fluid stable. In contrast, in the sitting position, the irrigation fluid tends to flow away from the surgical field, making stable ultrasound visualization more difficult. Nevertheless, the sitting position remains a valid and safe option in fully microscopic approaches when performed with standardized precautions.

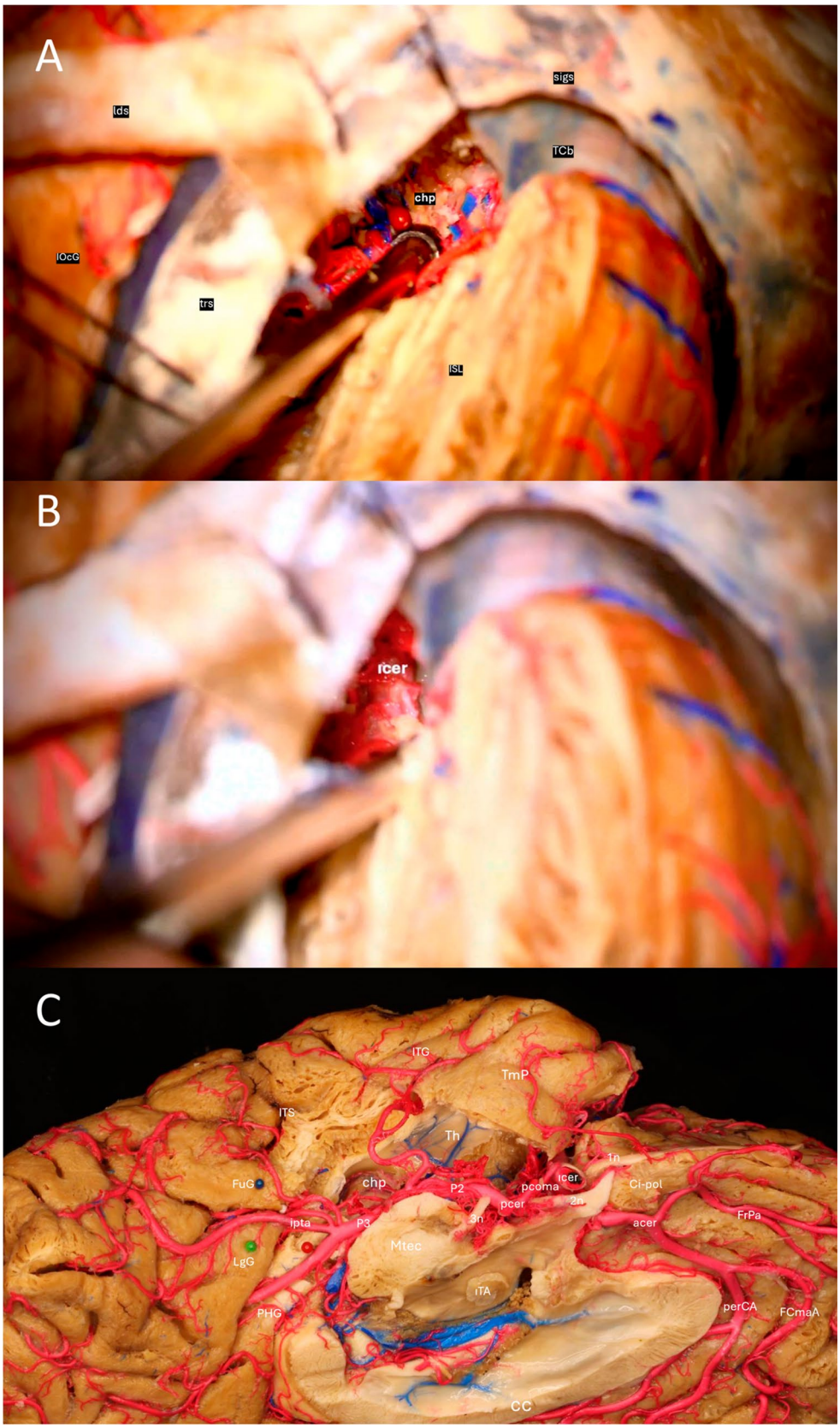

Fig. 6 (**A**) Resection of the hippocampus tail anteriorly, leaving the posterior cerebral artery P3 and P2 branches medially and the collateral sulcus laterally. After approximately 2.5 cm, resected the hippocampal body and head by moving superiorly and medially until reaching temporal horn, and visualization of choroid plexus with temporal horn lateral wall resection. During this procedure, approximately 2 cm^3 of the fusiform gyrus was resected to provide sufficient visual angle. (**B**) Resection of the amygdala and the remainder of the hippocampus head, continuing the dissection from the temporal horn lateral wall lateral and inferiorly until internal cerebral artery and optic nerve are seen. (**C**) After resection, the image of the inferior surface of the right hemisphere is removed. (CC; corpus callosum, chp; choroid plexus, CG; cingulat gyrus, cols; collateral sulcus, Ci-pol; cingulat pole, fug; fusiform gyrus, FCmaA; fronto callosomarginal artery, FrPa; frontopolar artery, GR; gyrus rectus, IOcG; inferior occipital gyrus, ITA; interthalamic adhesion, ITG; inferior temporal gyrus, ITS; inferior temporal sulcus, iata; inferior anterior temporal artery, icer; internal cerebral artery, ipta; inferior parieto-temporal artery, lgg; lingual gyrus, moca; medial occipital artery, Mtec; mesencephalic tectum, ocp; occipital pole, Org; orbital gyrus, perCA; pericallosal artery, PHG; parahippocampal gyrus, pcerc; posterior cerebral artery calcarine branch, pcerpo; posterior cerebral artery parieto-occipital branch, sigs; sigmoid sinus, TCb; tentorium cerebelli, Tmp; temporal pole, artery, trs; transvers sinus, Un, uncus, 2n; optic nerve)

Table 1 Results of measurements on cadavers and 100 brain MRIs without cranial pathology

Measurements		Cadavers (mean ± SD)	Individuals (mean ± SD)
ANGLE MEASUREMENTS	Tentorial Angle	36.88 ± 4.2	41.76 ± 6.8
	Occipital Angle	108.86 ± 4.1	114.7 ± 8.4
SURGICAL DISTANCE MEASUREMENTS	Distance between the REP and the IchP (mm)	68.93 ± 6.8	64.67 ± 6.08
	Distance between the REP and the Th (mm)	68.29 ± 6.6	63.84 ± 6.1
	Distance between the REP and the TmP (mm)	85.21 ± 5.8	88.22 ± 9.6

Table 2 Statistical results of measurements

Measurements	OA	REP-IchP	REP-Th	REP-TmP
TA	$r=0.973$, $p<0.001$	$r=0.305$, $p=0.02$	$r=0.301$, $p=0.02$	$r=0.358$, $p=0.01$
OA	-	$r=0.294$, $p=0.03$	$r=0.292$, $p=0.03$	$r=0.346$, $p=0.01$
REP-IchP	-	-	$r=0.996$, $p<0.001$	$r=0.798$, $p<0.001$
REP-Th	-	-	-	$r=0.790$, $p<0.001$

REP retrosigmoid entry point, *ichp* inferior choroidal point, *th* the most anterior part of the Temporal Horn visible on MRI images, *tmp* Temporal pole, *TA* tentorial angle, *OA* occipital angle

Table 3 Approaches to the mediobasal Temporal region

Approach	Surface
Transsylvian-transinsular	Superior Surface
Sulci and gyri on the lateral surface Anterior temporal lobectomy	Lateral Surface
Sulci and gyri on the basal surface	Basal Surface
Transsylvian-transcisternal Occipital interhemispheric Supracerebellar transtentorial	Medial Surface

In addition, several studies comparing midline and paramedian supracerebellar infratentorial (SCIT) approaches have demonstrated that the paramedian route may offer important advantages when extending the exposure toward the tentorium. Anatomical and clinical series have shown that the paramedian SCIT corridor allows wider operative angles, improved maneuverability, and reduced need for sacrificing bridging veins due to the natural displacement of the superior cerebellar surface [41, 42]. These characteristics suggest that paramedian SCIT extensions may provide a safer and more functional working corridor compared with classic midline approaches when planning a transtentorial trajectory.

Endoscopic support can significantly complement the retrosigmoid transtentorial approach, especially in regions where the microscope provides a limited line of sight. A 30° angled endoscope, in particular, offers the ability to look 'around the corner' and visualize the anterior mediobasal temporal structures more effectively. Despite these advantages, endoscopic visualization may rapidly deteriorate in the presence of heavy bleeding, which remains an important limitation of endoscopy-based assistance. Recent advances such as systems that display microscopic, endoscopic, and navigation views simultaneously in a picture-in-picture format have been shown to facilitate more intuitive orientation and may improve safety during deep-seated dissections [43, 44]. For these reasons, endoscopy should be considered a valuable adjunct rather than a replacement for microscopic dissection in selected RSTTA cases.

The RSTTA offers a shorter corridor to the MTR than PST. Comparisons in cadavers and 100 MRIs showed decreased mean distances with RSTTA from REP to TmP (10 cm reduced to 8.8 cm), to Th (6.8 cm to 6.3 cm), and to IchP (7.6 cm to 6.4 cm). The authors believe that this will provide easier access to the surgical field and reduce surgical fatigue.

Limitations

This study has several limitations. First, it is based on radiological measurements and cadaveric dissections, which do not fully replicate the dynamic conditions of live surgery. Factors such as brain shift, venous congestion, cerebrospinal fluid dynamics, and intraoperative tissue compliance may alter the surgical corridor in ways that cannot be captured in fixed specimens. Second, although angle- and distance-based correlations provide objective anatomical information, the absence of clinical cases prevents any conclusions regarding operative safety, complication profiles, or functional outcomes. Third, variations in tentorial configuration, venous anatomy, and temporal lobe morphology among different populations may limit the generalizability of the findings. Finally, all simulations were performed under standardized head positioning, and alternative positioning techniques or patient-specific constraints may influence the applicability of these measurements. Future clinical and intraoperative studies are needed to validate these anatomical observations in real surgical settings.

Conclusion

This study demonstrates that the retrosigmoid transtentorial approach provides a practical anatomical route to the mediobasal temporal region when tentorial and occipital angles are favorable. The correlations identified between

angular measurements and REP-based distances offer an objective framework for estimating the anterior extent of exposure and for anticipating when endoscopic assistance may be required. These findings contribute to a clearer understanding of the anatomical factors that influence the reach and applicability of the RSTTA. Nevertheless, clinical studies are needed to confirm the relevance of these anatomical observations in operative practice.

Author contributions M.E. conceived and designed the study, performed the cadaveric dissections, acquired and analyzed the radiological data, conducted the statistical analyses, and drafted the manuscript. U.T., N.Ç.K., M.E.A., M.Z., C.F.K., and M.H.Ş. contributed to the cadaveric dissections, anatomical evaluations, and acquisition of intraoperative and radiological measurements. S.K. assisted in the anatomical dissections and provided expert guidance on anatomical structures and dissection methodology. A.Y. reviewed all radiological measurements, verified imaging accuracy, and contributed to radiological interpretation. H.H.K. supervised the entire study, provided senior neurosurgical guidance during anatomical dissections and methodological development, and critically revised and refined the manuscript. All authors reviewed and approved the final version of the manuscript.

Funding This study was supported by the Scientific Research Projects (BAP) Unit of Erzurum Atatürk University.

Data availability The datasets generated and/or analyzed during the current study are available from the corresponding author on reasonable request.

Declarations

Ethics approval This study was performed as a scientific research project in the Erzurum Atatürk University Neuroanatomy Laboratory between 2022 and 2023, after receiving approval from the Ethics Committee of Erzurum Atatürk University (Approval code: TTU-2022-10480).

Consent to participate Not applicable (no human participants were directly involved).

Consent to publish Not applicable (no identifying information of participants is included in this article).

Competing interests The authors declare no competing interests.

References

1. Xu Y et al (2023) Medial Temporal Lobe Tumors: Surgical Anatomy and Technique. Functional Anatomy of the Brain: A View from the Surgeon's Eye, : pp. 299–320
2. Türe U et al (2012) The paramedian supracerebellar-transtentorial approach to the entire length of the mediobasal Temporal region: an anatomical and clinical study: laboratory investigation. J Neurosurg JNS 116(4):773–791
3. Lafazanos S et al (2015) Evaluating the importance of the tentorial angle in the paramedian supracerebellar-transtentorial approach for selective amygdalohippocampectomy. World Neurosurg 83(5):836–841
4. Campero A et al (2006) Microsurgical approaches to the medial Temporal region: an anatomical study. Neurosurgery 59(4 Suppl 2): ONS279-307; discussion ONS307-308
5. Germano IM (1996) Transsulcal approach to mesiotemporal lesions. Anatomy, technique, and report of three cases. Neurosurg Focus 1(5):e4
6. Vajkoczy P et al (1998) Modified approach for the selective treatment of Temporal lobe epilepsy: transsylvian-transcisternal mesial En bloc resection. J Neurosurg 88(5):855–862
7. Klingler J (1935) Erleichterung der makrokopischen Präparation des gehirns durch Den gefrierprozess. Orell Füssli
8. Velho V et al (2019) Lateral Semi-sitting position: A novel method of patient's head positioning in suboccipital retrosigmoid approaches. Asian J Neurosurg 14(1):82–86
9. Fish D, Andermann F, Olivier A (1991) Complex partial seizures and small posterior Temporal or extratemporal structural lesions: surgical management. Neurology 41:1781–1784
10. Spencer D, Spencer S, Spencer D (1991) Anteromedial temporal lobectomy: directing the surgical approach to the pathologic substrate. Blackwell Scientific, pp 129–137
11. Nascimento FA et al (2016) Anterior Temporal lobectomy versus selective amygdalohippocampectomy in patients with mesial Temporal lobe epilepsy. Arq Neuropsiquiatr 74(1):35–43
12. Srikijvilaikul T et al (2011) Outcome of Temporal lobectomy for hippocampal sclerosis in older patients. Seizure 20(4):276–279
13. Falowski SM et al (2012) Tailored temporal lobectomy for medically intractable epilepsy: evaluation of pathology and predictors of outcome. Neurosurgery 71(3):703-9; discussion 709
14. Iachinski RE et al (2014) Patient satisfaction with Temporal lobectomy/selective amygdalohippocampectomy for Temporal lobe epilepsy and its relationship with Engel classification and the side of lobectomy. Epilepsy Behav 31:377–380
15. Salanova V, Markand O, Worth R (2002) Temporal lobe epilepsy surgery: outcome, complications, and late mortality rate in 215 patients. Epilepsia 43(2):170–174
16. Sindou M et al (2006) Temporo-mesial epilepsy surgery: outcome and complications in 100 consecutive adult patients. Acta Neurochir (Wien) 148(1):39–45
17. Adam C et al (1996) Variability of presentation in medial Temporal lobe epilepsy: a study of 30 operated cases. Acta Neurol Scand 94(1):1–11
18. Fisch B (2011) Anterior Temporal lobectomy - how safe is it? Epilepsy Curr 11(6):186–188
19. Wieser H, Yaşargil M (1982) Selective amygdalohippocampectomy as a surgical treatment of mesiobasal limbic epilepsy. Surg Neurol 17:445–457
20. Yaşargil M et al (2010) The selective amygdalohippocampectomy for intractable Temporal limbic seizures. Historical vignette. J Neurosurg 112:168–185
21. Kadri PAS et al (2017) Surgical approaches to the Temporal horn: an anatomic analysis of white matter tract interruption. Operative Neurosurg 13(2):258–270
22. Yeni SN et al (2008) Visual field defects in selective amygdalohippocampectomy for hippocampal sclerosis: the fate of Meyer's loop during the transsylvian approach to the temporal horn. Neurosurgery 63(3):507–513; discussion 513–515
23. Delev D et al (2016) Vision after trans-sylvian or temporobasal selective amygdalohippocampectomy: a prospective randomised trial. Acta Neurochir 158(9):1757–1765
24. Schmeiser B et al (2017) Visual field defects following different resective procedures for mesiotemporal lobe epilepsy. Epilepsy Behav 76:39–45
25. Kim YB, Lee KS (2018) Subtemporal approach. Neurovascular surgery: surgical approaches for neurovascular diseases. Springer, Singapore Singapore, pp 35–41

26. Elhammady MS, Heros RC (2016) Temporal lobe venous preservation. J Neurosurg 124(2):429–431
27. Yaşargil M (1996) Microneurosurgery IVB. Georg Thieme
28. Smith K, Spetzler R (1995) Supratentorial-infraoccipital approach for posteromedial Temporal lobe lesions. J Neurosurg 82:940–944
29. Weiner H, Kelly P (1996) A novel computer-assisted volumetric stereotactic approach for resecting tumors of the posterior parahippocampal gyrus. J Neurosurg 85:272–277
30. Yaşargil M, Türe U, Yaşargil D (2004) Impact of Temporal lobe surgery. J Neurosurg 101:725–738
31. Marino R, Rasmussen T (1968) Visual field changes after Temporal lobectomy in man. Neurology 18:825–835
32. Mengesha T et al (2009) Visual field defects after selective amygdalohippocampectomy and standard Temporal lobectomy. J Neuroophthalmol 29(3):208–213
33. Falconer M, Wilson J (1958) Visual field changes following anterior Temporal lobectomy: their significance in relation to meyer's loop of the optic radiation. Brain 81:1–14
34. Xu K et al (2020) Comparisons of the seizure-free outcome and visual field deficits between anterior Temporal lobectomy and selective amygdalohippocampectomy: A systematic review and meta-analysis. Seizure 81:228–235
35. Tokugawa J et al (2015) Novel classification of the posterior auricular artery based on angiographical appearance. PLoS ONE 10(6):e0128723
36. Ammirati M et al (2013) A streamlined protocol for the use of the semi-sitting position in neurosurgery: a report on 48 consecutive procedures. J Clin Neurosci 20(1):32–34
37. Feigl GC et al (2014) Neurosurgical procedures in the semi-sitting position: evaluation of the risk of Paradoxical venous air embolism in patients with a patent foramen ovale. World Neurosurg 81(1):159–164
38. Jadik S et al (2009) A standardized protocol for the prevention of clinically relevant venous air embolism during neurosurgical interventions in the semisitting position. Neurosurgery 64(3):533–539
39. Choque-Velasquez J et al (2018) Praying sitting position for pineal region surgery: an efficient variant of a classic position in neurosurgery. World Neurosurg 113:e604–e611
40. Choque-Velasquez J et al (2018) Venous air embolisms and sitting position in Helsinki pineal region surgery. Surg Neurol Int 9:160
41. Choque-Velasquez J et al (2020) Midline and paramedian supracerebellar infratentorial approach to the pineal region: a comparative clinical study in 112 patients. World Neurosurg 137:e194–e207
42. Matsuo S et al (2016) Midline and off-midline infratentorial supracerebellar approaches to the pineal gland. J Neurosurg 126(6):1984–1994
43. Salma A, Ammirati M (2012) Real time parallel intraoperative integration of endoscopic, microscopic, and navigation images: a proof of concept based on laboratory dissections. J Neurol Surg Part B: Skull Base 73(01):036–041
44. Colasanti R et al (2016) Expanding the horizon of the suboccipital retrosigmoid approach to the middle incisural space by cutting the tentorium cerebelli: anatomic study and illustration of 2 cases. World Neurosurg 92:303–312